Biotechnology and Bioprocess Engineering 23: 11-15 (2018)
DOI 10.1007/s12257-017-0451-2

pISSN 1226-8372
eISSN 1976-3816

RESEARCH PAPER

R5 Peptide-based Biosilicification Using Methyltrimethoxysilane

Jeong Chan Park, Do Hyeon Kim, Chang Sup Kim, and Jeong Hyun Seo

Received: 7 November 2017 / Revised: 2 January 2018 / Accepted: 18 January 2018

Abstract We examined the performance of methyltrimethoxysilane (MTMS), a precursor of silicic acid, in the process of biosilicification induced by the R5 peptide from *Cylindrotheca fusiformis*. Recombinant GFP-R5 fusion protein was produced by *Escherichia coli* cultured at 25°C as a soluble and functional formation, but not at 37°C. MTMS-based biosilica deposits had a larger average diameter compared to tetraethyl orthosilicate (TEOS)-based deposits. Reducing phosphate concentration in the buffer system led to a decrease in the size of MTMS-based biosilica. These results provide insight into the surface modification of biosilica, and control of biosilica particle size, when using hydrophobic precursors such as MTMS.

Keywords: methyltrimethoxysilane, biosilica, hydrophobic silane, GFP-R5 fusion system

1. Introduction

Silica, which is an oxidized form of silicon (Si), has great utility in many industrial and biological applications [1,2]. Fabrication of silica particles *via* classical routes has been conducted under harsh reaction conditions, such as high or low pH, high reaction temperature, using harmful chemicals, or with long reaction times at room temperature. These conditions often reduce (or completely block) the activity of biomolecules.

Biosilica formation has been receiving great attention because of the ecofriendly and biocompatible reaction conditions for biotechnology applications [3,4]. R5 peptide, which is one of the repeating units of a silaffin protein found in silica cell walls of the diatom *Cylindrotheca fusiformis*, can induce rapid precipitation of silica under biologically compatible conditions [5]. In addition, an R5-enzyme fusion strategy has been used to enhance thermostability and improve recovery of the enzyme [3].

Biosilicification of R5 or R5-fused proteins has been generally performed with tetramethyl orthosilicate (TMOS), tetraethyl orthosilicate (TEOS) and a mixture of other functionalized silanes as precursors of silicic acid [6,7]. The use of different precursor types, imparts diverse functionalities to the silica particles. In addition, the use of silanes with hydrophobic groups allows the regulation of silica particles hydrophobicity; this is useful for many applications such as the entrapment of enzymes with hydrophobic domain, hydrophobic drug delivery systems and biosensor that require hydrophobic silica [8,9]. Here, we studied the effect of a silica precursor, methyltrimethoxysilane (MTMS), during the process of biosilicification. MTMS has one non-hydrolysable methyl group and three hydrolysable methoxy groups. The three methoxy groups are hydrolyzed, giving rise to hydroxyl groups. As the condensation reaction and polymerization proceeds, the number of hydrophobic methyl groups increases compared to that of hydrophilic hydroxyl groups, conferring hydrophobic properties on the product [10]. MTMS is usually employed for the preparation of silica-based aerogel through the sol-gel process [2,11]. However, there are limited reports of MTMS-based R5 biosilica formation [7]. Using green fluorescent protein

Jeong Chan Park†
Department of Chemical Engineering, Pohang University of Science and Technology, Pohang 790-784, Korea

Do Hyeon Kim†, Jeong Hyun Seo*
School of Chemical Engineering, Yeungnam University, Gyeongsan 38541, Korea
Tel: +82-53-810-2525; Fax: +82-53-810-4631
E-mail: jhseo78@yu.ac.kr

Chang Sup Kim
School of Chemistry and Biochemistry, Yeungnam University, Gyeongsan 38541, Korea

†These authors contributed equally to this work.

(GFP) as a model protein [12], we herein demonstrate MTMS-mediated biosilica formation *via* R5. The process can be easily monitored owing to production of the fluorescent signal [13,14]. In addition, we evaluated the impact of different buffer systems on the biosilicification of MTMS-based GFP-R5.

2. Materials and Methods

2.1. Vector construction

The GFP gene was polymerase chain reaction (PCR)-amplified from pTrc-HisC-GFP vector [15] (forward primer 5′-GCGCCATATGAGTAAAGGAGAAGAACTTTT-3′ and reverse primer 5′-TATAAGCTTTTTGTAGAGCTCATC CATGCC-3′). The PCR product was digested using *Nde*I and *Hind*III. After removing the *ng*CA gene from pET-*ng*CA-R5, a vector we constructed previously [6], the digested GFP fragment was subcloned, resulting in pET-GFP-R5. The fusion DNA sequence was verified by direct sequencing. *Escherichia coli* BL21 (DE) (Novagen, Wisconsin, USA) was grown at 37°C in Luria-Bertani (LB) media and transformed with pET-GFP-R5. The optical density of the bacterial cultures was measured using a 96-well microplate reader (SPECTROstar Nano®, BMG Labtech, Ortenberg, Germany) at 600 nm. The GFP expression level of the cells was monitored by measuring the fluorescence intensity using a spectrofluorophotometer (RF-5301PC, Shimadzu, Kyoto, Japan) at an excitation wavelength of 395 nm, emission wavelength of 509 nm, and emission slit width of 3 nm.

2.2. Expression of GFP-R5 fusion protein

Medium containing *E. coli* BL21 (DE) transformed with pET-GFP-R5 (1 mL) was used to inoculate 50 mL of LB media containing ampicillin (USB, Salem, USA), and cultures were incubated until they reached an OD_{600} of approximately 0.9. Expression of the recombinant fusion protein was induced by adding 50 μL of 1 M isopropyl-β-D-thiogalactopyranoside (IPTG; Carbosynth, Berkshire, UK) to the cell media. Then, the cell solutions were incubated for 24 h at 37 or 25°C, monitoring the cell growth and expression level of GFP-R5 protein with measurement of OD_{600} values and the fluorescence intensity (FI) (excitation wavelength: 395 nm and emission wavelength: 509 nm), respectively.

2.3. Purification of recombinant fusion protein and SDS-PAGE analysis

For the protein purification, the cell solutions were incubated for 24 h and then collected by centrifugation. The harvested cells were suspended in lysis buffer (50 mM NaH_2PO_4, 300 mM NaCl and 10 mM imidazole; pH 8) containing a final concentration of 1 mM phenylmethylsulfonyl fluoride (PMSF) as a protease inhibitor and sonicated (3 sec pulse on and 10 sec pulse off, 35% amplitude). The cell debris was removed by centrifugation (400 × *g*, 10 min) to collect the supernatant, designated as the cell lysate. The cell lysate was centrifuged at 10,000 × *g* (10 min) to collect supernatant, which was designated as the soluble fraction. The remaining pellet was designated as the insoluble fraction. The soluble fraction was subjected to affinity chromatography using Ni-nitrilotriacetic acid (NTA) agarose beads (Qiagen, Hilden, Germany) for recombinant fusion protein purification. The loaded protein was washed with 20 mM imidazole lysis buffer and eluted with 250 mM imidazole lysis buffer. The eluted fusion protein was dialyzed against 50 or 10 mM PBS buffer for further experiments.

The cell lysate, soluble fraction, insoluble fraction, and purified fusion protein were subjected to sodium dodecyl sulfate-polyacrylamide gel electrophoresis (SDS-PAGE). The gel was stained with Coomassie Brilliant Blue G-250 (Bio-Rad, Hercules, USA).

2.4. Silica encapsulation and electron microscopy analysis

Tetraethyl orthosilicate (TEOS, Sigma-Aldrich, St. Louis, USA, 1 M) or methyltrimethoxy silane (MTMS, Sigma-Aldrich, St. Louis, USA, 1 M), a precursor of silicic acid, was hydrolyzed in 1 mM hydrochloric acid solution (dilution with water or ethanol). Biosilica formation was performed by mixing 20 μL of purified GFP-R5 protein (10 mg/mL) in 50 or 10 mM PBS buffer with 160 μL of PBS buffer and 20 μL of 1 M silane solutions for 10 sec or 30 min. For scanning electron microscopy (SEM, Hitachi S-4200), samples were mounted on carbon tapes. The samples were dried in a 60°C dry oven, washed with deionized water, and then dried again.

3. Results and Discussion

We explored the formation of biosilica particles mediated by GFP-R5 proteins in the presence of TEOS or MTMS. Amino groups of R5 would interact with hydroxyl groups of silicic acids and facilitate the polycondensation reaction, leading to silica precipitation (Fig. 1) [5]. As shown in Fig. 2, the R5 peptide sequence was genetically fused to the C-terminus of GFP gene with a His_6-tag provided by the parental vector, resulting in pET-GFP-R5. The pET-GFP-R5 transformed *E. coli* BL21 (DE) were grown at 37 or 25°C (hereafter 'GFP-R5-37' and 'GFP-R5-25', respectively).

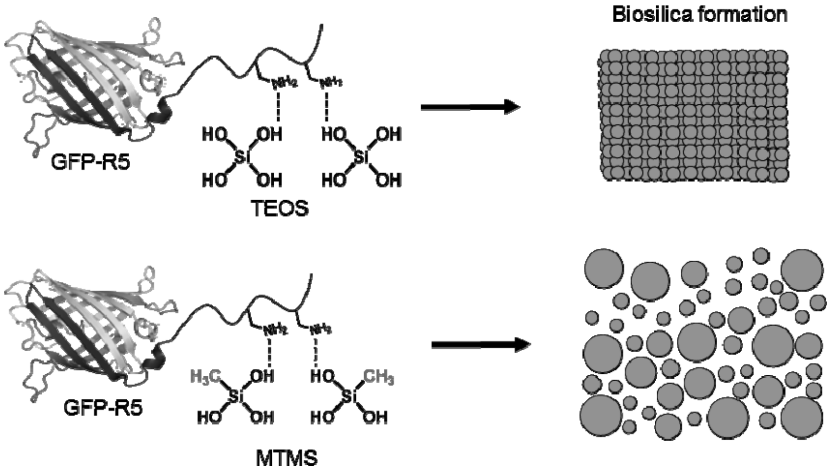

Fig. 1. Schematic representation of biosilica formation mediated by GFP-R5 fusion protein in the presence of TEOS or MTMS.

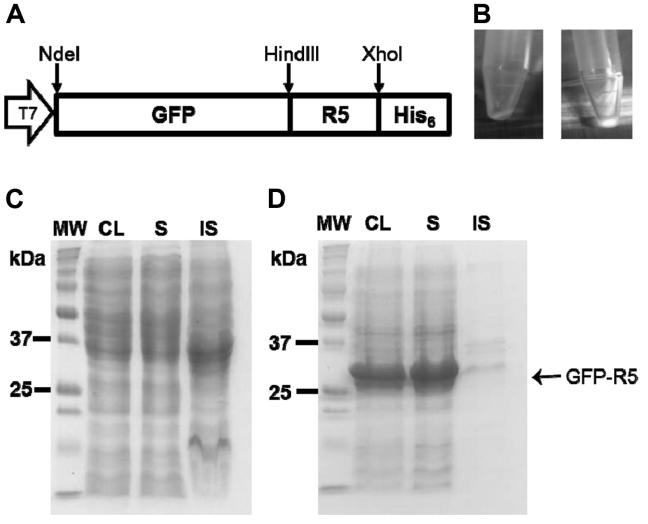

Fig. 2. (A) Construction of the plasmid encoding the GFP-R5 fusion protein. (B) Fluorescence signal of GFP-R5 transformed *E. coli* BL21 (DE) grown at 37°C (left) and 25°C (right), respectively. SDS-PAGE of the cell lysate (CL), soluble (S), and insoluble (IS) fraction of GFP-R5 transformed *E. coli* BL21 (DE) grown at (C) 37°C and (D) 25°C, respectively.

Whereas the fluorescence of GFP-R5-37 was not detectable, a bright fluorescence signal was observed with GFP-R5-25, as shown in Fig. 2B. Cell lysate, and soluble or insoluble fractions of GFP-R5-37 and GFP-R5-25 were also analyzed by gel electrophoresis. The recombinant fusion protein, GFP-R5, was detected in both the cell lysate and soluble fraction of GFP-R5-25 (Fig. 2D), indicating that the recombinant protein is overexpressed as a soluble form in *E. coli*, and is stable at 25°C.

The growth of GFP-R5-expressing *E. coli* was monitored by measuring the optical density (Fig. 3A), and the typical lag and exponential phases of bacterial growth were observed. Protein expression level was also assessed by measuring the fluorescence intensity (FI) of GFP. The pattern of the FI curve was similar to that of the growth curve. The soluble fraction of the cell lysate was loaded on SDS-PAGE, revealing that the profile of the soluble fraction from the cell lysate was consistent with the growth and FI curves (Fig. 3B). Fusion proteins were subsequently purified using His_6-tag metal affinity chromatography (Fig. 3C).

To examine whether the GFP-R5 fusion system remained amenable to silica formation, we added TEOS to initiate the process. Silica particles with an average diameter of 605 nm formed and then aggregated, as shown in Fig. 4A. In the case of MTMS, connected silica particles were obtained (Fig. 4B). The same phenomenon, which is connected into large clusters, has been observed in the context of MTMS-modified SiO_2 particles [16]. The size of MTMS-based biosilica was in the microscale range (an average size of 1.05 μm). When the reaction time increased from 10 sec to 30 min, MTMS-based biosilica particles with an average size of 974 nm formed and were separated; this size was similar that of biosilica formed over a shorter reaction time (10 sec) (Fig. 4C). The average sizes of biosilica particles were obtained from TEM image analysis. We next investigated the effect of buffer phosphate concentration on MTMS-mediated biosilica formation, since phosphate anions are reported to be a prerequisite for silica formation, and are critical determinants of the size [17]. Phosphate anions in phosphorylated silaffins serve as ionic cross-linkers causing the aggregation of cationic silaffin molecules [18]. In our reaction conditions, reducing the phosphate concentration from 50 to 10 mM, was concomitant with a reduction in the size of MTMS-based biosilica deposits

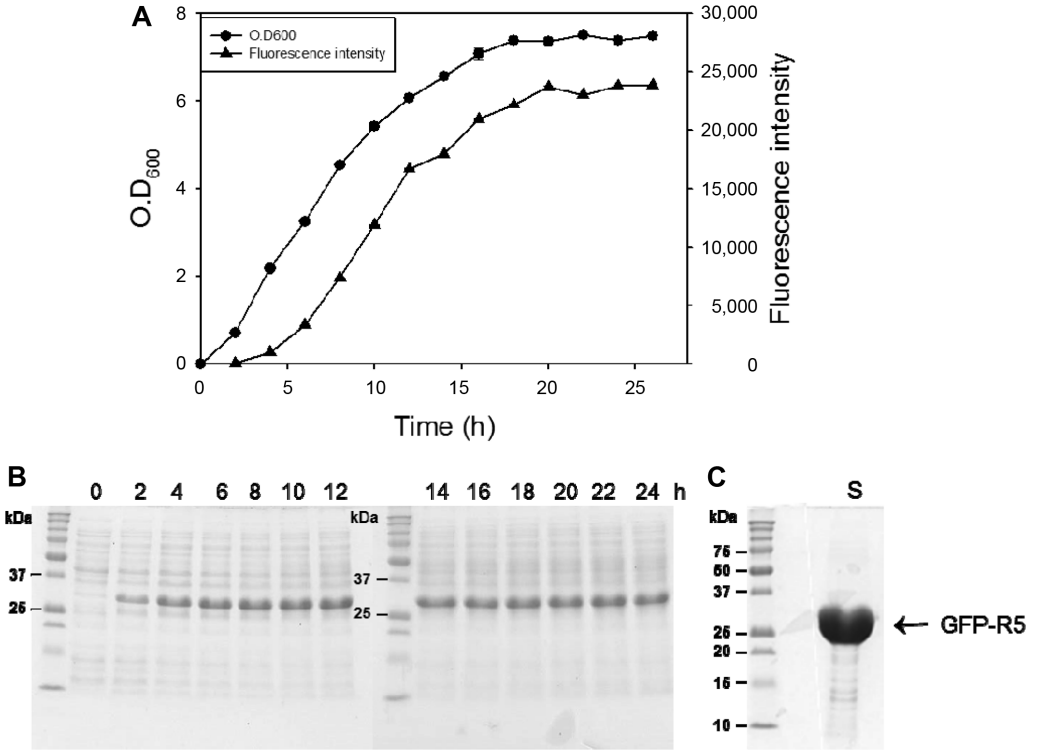

Fig. 3. Monitoring of (A) cell growth and expression level of GFP-R5 protein in *E. coli*. (B) SDS-PAGE profiles of the transformed *E. coli* over 24 h. (C) SDS-PAGE of GFP-R5 fusion proteins.

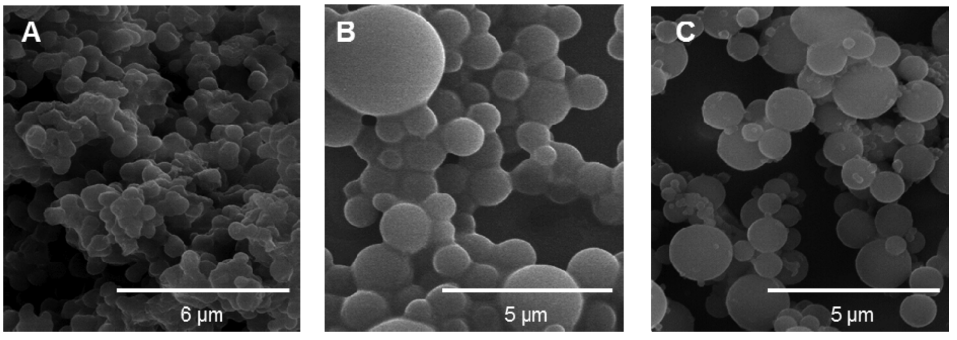

Fig. 4. SEM images of biosilica of GFP-R5 in the presence of (A) TEOS and (B) MTMS following reaction times lasting 10 sec. (C) SEM image of MTMS-based biosilica with 30-min reaction times.

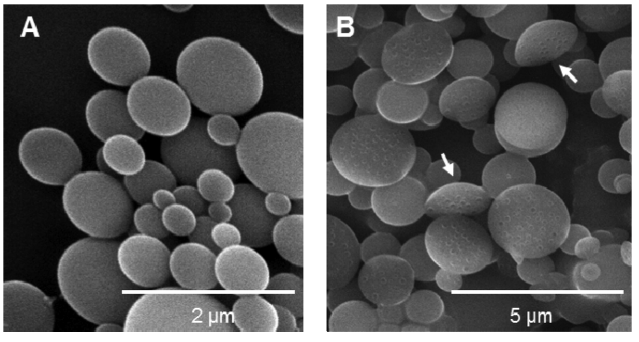

Fig. 5. SEM images of biosilica of GFP-R5 in different buffer systems. (A) 10 mM phosphate buffer and (B) 1:9 (v/v) ratio of ethanol : 50 mM phosphate buffer. Arrows indicate the rugby ball-shaped silica particles.

(from 974 to 623 nm, Fig. 5A). This observation is consistent with reported results of mono- and disilicic acid-based biosilica formation mediated by polyamines [17], and suggests that MTMS solution properties are impacted by phosphate anions in a manner similar to that observed with other silica precursors. In an additional test of buffer conditions, MTMS was hydrolyzed in ethanol and then mixed with 50 mM phosphate buffer (ethanol:phosphate buffer ratio 1:9 v/v). Interestingly, some of the biosilica particles adopted the shape of 'rugby balls' with 1.4-μm average diameters (Fig. 5B). These results imply that the components of the reaction buffer system will influence the size and morphology of particles formed as a result of

MTMS-based biosilicification. Further studies will be required to fully optimize the conditions for the control of MTMS-initiated biosilicification.

4. Conclusion

Here, using a GFP-R5 fusion system, we demonstrated the feasibility of MTMS-based biosilica formation. Our key finding was that the size of MTMS-dependent biosilica particles decreased concomitantly with a reduction in the concentration of phosphate anions in the reaction buffer system. Our results may guide further research into the surface modification of biosilicification using hydrophobic silanes, and the regulation of particle size using an MTMS-based biosilicification approach.

Acknowledgements

This study was supported by the 2017 Yeungnam University Research Grant and by the Human Resources Program in Energy Technology of the Korea Institute of Energy Technology Evaluation and Planning (KETEP) granted financial resource from the Ministry of Trade, Industry & Energy, Korea (No. 20174030201760).

References

1. Davis, M. E. (2002) Ordered porous materials for emerging applications. *Nature* 417: 813-821.
2. Sinkó, K. (2010) Influence of chemical conditions on the nanoporous structure of silicate aerogels. *Materials* 3: 704-740.
3. Jo, B. H., C. S. Kim, Y. K. Jo, H. Cheong, and H. J. Cha (2016) Recent developments and applications of bioinspired silicification. *Kor. J. Chem. Eng*. 33: 1125-1133.
4. Betancor, L. and H. R. Luckarift (2008) Bioinspired enzyme encapsulation for biocatalysis. *Trends Biotechnol.* 26: 566-572.
5. Lechner, C. C. and C. F. Becker (2014) A sequence-function analysis of the silica precipitating silaffin R5 peptide. *J. Pept. Sci*. 20: 152-158.
6. Jo, B. H., J. H. Seo, Y. J. Yang, K. Baek, Y. S. Choi, S. P. Pack, S. H. Oh, and H. J. Cha (2014) Bioinspired silica nanocomposite with autoencapsulated carbonic anhydrase as a robust biocatalyst for CO_2 sequestration. *ACS Catal*. 4: 4332-4340.
7. Kuan, I. -C., C. -A. Chuang, S. -L. Lee, and C. -Y. Yu (2012) Alkyl-substituted methoxysilanes enhance the activity and stability of d-amino acid oxidase encapsulated in biomimetic silica. *Biotechnol. Lett*. 34: 1493-1498.
8. Gill, I. and A. Ballesteros (2000) Bioencapsulation within synthetic polymers (Part 1): sol–gel encapsulated biologicals. *Trends Biotechnol*. 18: 282-296.
9. Reetz, M. T. (1997) Entrapment of biocatalysts in hydrophobic sol-gel materials for use in organic chemistry. *Adv. Mater*. 9: 943-954.
10. Rao, A. V., S. D. Bhagat, H. Hirashima, and G. Pajonk (2006) Synthesis of flexible silica aerogels using methyltrimethoxysilane (MTMS) precursor. *J. Colloid Interf. Sci*. 300: 279-285.
11. Du, M., N. Mao, and S. Russell (2016) Control of porous structure in flexible silicone aerogels produced from methyltrimethoxysilane (MTMS): The effect of precursor concentration in sol–gel solutions. *J. Mater. Sci*. 51: 719-731.
12. Nam, D. H., K. Won, Y. H. Kim, and B. I. Sang (2009) A novel route for immobilization of proteins to silica particles incorporating silaffin domains. *Biotechnol. Prog*. 25: 1643-1649.
13. Park, J. C., G. T. Lee, C. S. Kim, and J. H. Seo (2017) Effects of surface charge and ligand type of Au nanoparticles on green fluorescent protein-expressing *Escherichia coli*. *Biotechnol. Bioproc. Eng*. 22: 83-88.
14. Kim, D. H., J. C. Park, G. E. Jeon, C. S. Kim, and J. H. Seo (2017) Effect of the size and shape of silver nanoparticles on bacterial growth and metabolism by monitoring optical density and fluorescence intensity. *Biotechnol. Bioproc. Eng*. 22: 210-217.
15. Song, Y. H., C. S. Kim, and J. H. Seo (2016) Noninvasive monitoring of environmental toxicity through green fluorescent protein expressing *Escherichia coli*. *Kor. J. Chem. Eng.* 33: 1331-1336.
16. Philipavičius, J., I. Kazadojev, A. Beganskienė, A. Melninkaitis, V. Sirutkaitis, and A. Kareiva (2008) Hydrophobic antireflective silica coatings *via* sol-gel process. *Mater. Sci*. 14: 283-287.
17. Sumper, M., S. Lorenz, and E. Brunner (2003) Biomimetic control of size in the polyamine-directed formation of silica nanospheres. *Angew. Chem. In. Ed*. 42: 5192-5195.
18. Kröger, N., S. Lorenz, E. Brunner, and M. Sumper (2002) Self-assembly of highly phosphorylated silaffins and their function in biosilica morphogenesis. *Sci*. 298: 584-586.